

NOMA Inspired Integrated Sensing and Communication

Zhaolin Wang, *Graduate Student Member, IEEE*, Xidong Mu, *Graduate Student Member, IEEE*,
Yuanwei Liu, *Senior Member, IEEE*, Zhiguo Ding, *Fellow, IEEE*

Abstract—A non-orthogonal multiple access (NOMA)-inspired integrated sensing and communication (ISAC) framework is proposed, where a dual-functional base station (BS) transmits the composite unicast communication signal and sensing signal. In contrast to treating the sensing signal as the harmful interference to communication, in this work, multiple beams of the sensing signal are employed to convey multicast information following the concept of NOMA. Then, each communication user receives multiple multicast streams and one desired unicast stream, which are detected with the aid of successive interference cancellation (SIC). Based on the proposed framework, a multiple-objective optimization problem (MOOP) is formulated for designing the transmit beamforming subject to the total transmit power constraint, which characterizes the trade-off between the communication throughput and sensing beampattern accuracy. For the general multiple-user scenario, the formulated MOOP is firstly converted to a single-objective optimization problem (SOOP) via the ϵ -constraint method. Then, a double-layer block coordinate descent (BCD) algorithm is proposed by employing fractional programming (FP) and successive convex approximation (SCA) to find a high-quality suboptimal solution. For the special single-user scenario, the globally optimal solution can be obtained by transforming the MOOP to a convex quadratic semidefinite program (QSDP). Moreover, it is rigorously proved that 1) in the multiple-user scenario, the proposed NOMA-inspired ISAC framework always outperform the state-of-the-art sensing-interference-cancellation (SenIC) ISAC frameworks by further exploiting sensing signal for delivering information; 2) in the special single-user scenario, the proposed NOMA-inspired ISAC framework achieves the same performance as the existing SenIC ISAC frameworks, which reveals that the coordination of sensing interference is not necessarily required in this case. Numerical results verify the theoretical results and show that exploiting one beam of the sensing signal for delivering multicast information is sufficient for the proposed NOMA-inspired ISAC framework.

Index Terms—Beamforming design, integrated sensing and communication (ISAC), multicast-unicast communication, non-orthogonal multiple access (NOMA).

I. INTRODUCTION

The beyond fifth generation (B5G) and sixth generation (6G) wireless networks are envisaged to enable a host of emerging applications like unmanned aerial vehicles (UAVs), autonomous driving, virtual and augmented reality, Internet

of vehicles, and smart city [2]. Therefore, in contrast to the past five generations of wireless networks that mainly support wireless communication, the B5G and 6G require a paradigm shift to the integration of multiple functions including communications, sensing, control, and computing [3]. Based on this vision, the concept of integrated sensing and communication (ISAC)¹ has emerged and attracted growing attention in both academia [4], [5] and industries [6], [7]. The goal of ISAC is to integrate the communication and radar sensing via the same platform and the same spectrum, which is capable of increasing resource efficiency and achieving mutual benefits. On the one hand, the resources for communication and radar sensing are shared in the ISAC, thus improving the utilization efficiency in terms of spectrum, hardware, energy, and costs [4]. On the other hand, the two functions can be interplayed with each other for realizing the win-win operations, such as the sensing-assisted pilot-free communication channel estimation [5] and the communication-assisted high-precision sensing [4].

A. Prior Works

Due to the resource sharing between the two functions of communication and radar sensing, there is a natural performance trade-off in ISAC. Therefore, the bound of the performance trade-off between the communication and radar sensing was investigated in [8] from the information-theoretic perspective, where the radar estimation rate was developed based on the rate distortion theory to unify the metrics of the communication and radar sensing. The authors of [9] introduced the concept of radar capacity based on the Hartley capacity measure and investigated the total communication-radar capacity of the integrated system. Waveform design is another research aspect and plays a key role for ISAC to achieve the harmony resource sharing and integration gain [4]. Early works of the waveform design in ISAC focused on the single-antenna systems. For instance, the authors of [10] designed a joint waveform for supporting the communication and radar sensing in a time-division manner, where the trapezoidal frequency-modulated continuous waveform was exploited for radar sensing in the radar cycle while the modulated single frequency carrier appeared in the communication cycle. In addition, the potential of the linear frequency modulated (LFM) waveform and orthogonal frequency division modulated (OFDM) waveform for ISAC was investigated in [11] and [12], respectively.

¹Note that the “sensing” in ISAC refers to radar sensing.

Part of this paper has been submitted to IEEE International Conference on Communications (ICC), Seoul, South Korea, May 16-20, 2022 [1].

Zhaolin Wang and Yuanwei Liu are with the School of Electronic Engineering and Computer Science, Queen Mary University of London, London E1 4NS, U.K. (e-mail: zhaolin.wang@qmul.ac.uk, yuanwei.liu@qmul.ac.uk).

Xidong Mu is with the School of Artificial Intelligence, Beijing University of Posts and Telecommunications, Beijing 100876, China (e-mail: muxidong@bupt.edu.cn).

Zhiguo Ding is with the School of Electrical and Electronic Engineering, The University of Manchester, Manchester M13 9PL, UK (e-mail: zhiguo.ding@manchester.ac.uk).

Given the limitations of the single-antenna technique, the multiple-antenna technique, which has been respectively successfully employed in both communication [13] and radar sensing [14], is adopted in the recent research contributions on ISAC. By exploiting spatial degrees of freedom (DoFs) provided by the multiple-antenna technique, different beams can be generated to carry out multiple-user communication and the multiple-target sensing. For example, the authors of [15] proposed two strategies for facilitating ISAC, namely the separated deployment and the share deployment, where the transmit beamforming in each deployment was designed to achieve the high-quality sensing beampattern while satisfying the minimum communication requirement. As a further research of the shared deployment, the closed-form optimal transmission beamforming for minimizing the inter-user interference subject to different radar sensing criteria was derived in [16], based on which the communication and radar sensing performance trade-off was investigated. Moreover, the authors of [17] introduced a general Pareto optimization framework and proposed a bisection algorithm to find the optimal trade-off point of the communication and radar sensing in terms of signal-to-interference-and-noise ratio (SINR) and difference between peak and sidelobe (DPSL), respectively. Most recently, the application of non-orthogonal multiple access (NOMA) in ISAC system was investigated in [18], where multiple communication users are supported via superposition coding (SC) and successive interference cancellation (SIC). The authors of [19] considered a more sophisticated application scenario of NOMA in ISAC, i.e., sensing targets require the multicast messages from the BS, which can be non-orthogonally superimposed and transmitted simultaneously with the unicast messages for communication users.

However, only communication signal was exploited in [15]–[19] for facilitating ISAC. Despite having the advantage that no additional interference is received at the communication users, it may lead to sensing beampattern distortion due to the lack of transmit DoFs, especially when the number of communication users is less than the number of transmit antennas [20]. As a remedy, the authors of [20] proposed to employ extra dedicated sensing signals to provide full transmit DoFs for radar sensing. The authors of [21] also employed the dedicated sensing signals to generate the full-rank transmit covariance matrix, which is exploited to estimate the parameters of the extended target via the maximum likelihood estimation. In [22], the optimal transmit beamforming design is studied, where it is proved and demonstrated that cancelling the interference from sensing signal to communication can significantly improve the ISAC performance. As a further advance, the application of the dirty paper coding (DPC) for interference management of communication and sensing signals was investigated in [23].

B. Motivation and Contribution

Compared to the system which merely employs the communication signals for achieving the two functions, it has been shown that additional dedicated sensing signals are

generally essential to better facilitate sensing in ISAC [20]–[22]. This, however, also causes significant challenges in how to coordinate the sensing signals for supporting communications. In the existing ISAC frameworks, the sensing signal is regarded as the harmful interference to communication, which is mitigated through the beamforming design [20], [21] or the ideal interference-cancellation receiver [22]. To the best of the authors’ knowledge, the potentials of exploiting the sensing signal to further convey information for benefiting the communication have not been investigated. This provides the main motivation of this work.

Note that the superposition of the communication and sensing signals in ISAC is a kind of *non-orthogonal* resource sharing, which shares a similar idea with NOMA [24], [25]. For NOMA, the information-bearing signals are superimposed at the transmitter and the co-channel interference is partially or totally eliminated by the SIC at the receiver [26]. Although there have been some works of interplay between NOMA and ISAC [18] and [19], they mainly focused on exploiting NOMA to achieve multiple access of different kinds of communication user. However, in this work, we go beyond the scope of multiple access and aim to use the principle of NOMA to coordinate the communication signal and the sensing signal. Based on this idea, we propose a NOMA-inspired ISAC framework. The key principle is that the sensing signal is further exploited for multicast transmission and added on the unicast communication signal at the BS following NOMA. The main benefits of the proposed NOMA-inspired ISAC framework are summarized as follows. On the one hand, as the sensing signal is information-bearing, SIC can be employed at the communication users to remove the interference suffering from the sensing signal before decoding their unicast communication signals. On the other hand, the sensing signal is not only used for radar sensing but also used for delivering extra multicast information, thus benefiting communications and facilitating the sophisticated network operations. Based on this framework, we investigate the corresponding transmit beamforming design problems and the communication-sensing trade-off. The main contributions of this work are summarized below, which are boldly and explicitly contrasted to the state-of-the-art in Table I.

- We propose a novel NOMA-inspired ISAC framework, where a dual-functional base station (BS) transmits the multicast-information-bearing sensing signal and the unicast communication signals based on the concept of NOMA. The sensing signal is exploited for both multicast transmission and radar sensing and its interference at the communication users is eliminated via SIC. To investigate the fundamental trade-off between communication and radar sensing, we formulate a multiple-objective optimization problem (MOOP) of the communication throughput and the sensing beampattern matching error subject to the total transmit power constraint.
- For the multiple-user scenario, we convert the formulated MOOP to a single-objective optimization problem (SOOP) via the ϵ -constraint method. To solve the resultant non-convex SOOP, we propose a double-layer block

TABLE I: Our contributions compared with the state-of-the-art

	[15]–[17]	[18], [19]	[20], [21]	[22]	Our work
Communication signal	✓	✓	✓	✓	✓
Sensing signal	×	×	✓	✓	✓
Sensing interference cancellation	×	×	×	✓	✓
Sensing signal for communication	×	×	×	×	✓
The role of NOMA	×	facilitating multiple-user communication	×	×	facilitating coordination of communication and sensing signals

coordinate descent (BCD) algorithm employing fractional programming (FP) and successive convex approximation (SCA) to obtain a suboptimal solution.

- For the special single-user scenario, we reformulate the communication throughput and convert the related MOOP to a quadratic semidefinite program (QSDP) by employing the ϵ -constraint method, which is shown to be convex and can be globally optimally solved.
- We theoretically prove that for achieving the same radar sensing performance, the proposed framework can enhance the communication performance compared to the existing sensing-interference-cancellation (SenIC) ISAC frameworks in the multiple-user scenario. Moreover, for the single-user scenario, we rigorously prove that the performance achieved by all schemes becomes the same, indicating that the sensing interference coordination is not needed in this case.
- Our numerical results verify that in comparison to the existing ISAC framework, the proposed NOMA-inspired ISAC framework achieves larger trade-off region and better transmit beam pattern for sensing in the multiple-user scenario, while have the same performance in the single-user scenario. Furthermore, it also shows that in the proposed framework, exploiting only one beam of the sensing signal for the multicast transmission is sufficient to achieve the maximum communication throughput.

C. Organization and Notation

The rest of this paper is organized as follows. In Section II, the proposed NOMA-inspired ISAC framework is presented. Then, a MOOP of transmit beamforming between communication throughput and sensing beam pattern accuracy is formulated. In Section III, a suboptimal solution of the formulated problem in the general multiple-user scenario is obtained by the proposed double-layer FP-SCA-based BCD algorithm, while a globally optimal solution in the special single-user scenario is obtained via QSDP. Then, the properties of the proposed framework are studied for the two scenarios in comparison to the state-of-the-art ISAC frameworks. In Section IV, the numerical results are presented to characterize the proposed NOMA-inspired ISAC framework. Finally, this paper is concluded in Section V.

Notations: Scalars, vectors, and matrices are denoted by the lower-case, bold-face lower-case, and bold-face upper-case letters, respectively; $\mathbb{C}^{N \times M}$ and $\mathbb{R}^{N \times M}$ denotes the space of $N \times M$ complex and real matrices, respectively; a^* and $|a|$ denote the conjugate and magnitude of scalar a ; \mathbf{a}^H

denotes the conjugate transpose of vector \mathbf{a} ; $\mathbf{A} \succeq 0$ means that matrix \mathbf{A} is positive semidefinite; $\text{rank}(\mathbf{A})$, $\|\mathbf{A}\|_*$, and $\|\mathbf{A}\|_2$ denote the rank, nuclear norm, and spectral norm of matrix \mathbf{A} , respectively; $\mathbb{E}[\cdot]$ denotes the statistical expectation; $\mathcal{CN}(\mu, \sigma^2)$ denotes the distribution of a circularly symmetric complex Gaussian (CSCG) random variable with mean μ and variance σ^2 .

II. SYSTEM MODEL AND PROBLEM FORMULATION

A. System Model

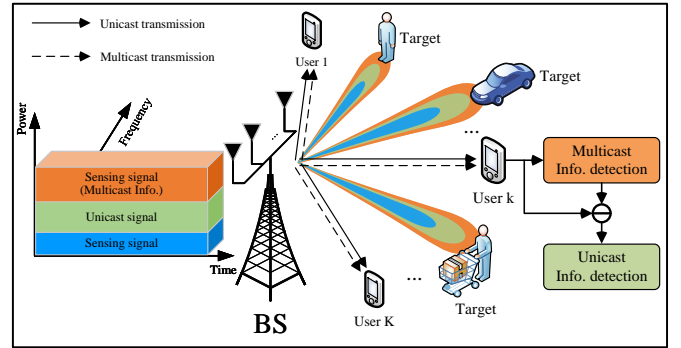


Fig. 1: Illustration of the proposed NOMA-inspired ISAC framework.

As shown in Fig. 1, a NOMA-inspired ISAC framework is proposed, which consists of a dual-functional N -antenna BS, K single-antenna communication users indexed by $\mathcal{K} = \{1, \dots, K\}$, and multiple radar sensing targets. For delivering the unicast information symbol $s_k \in \mathbb{C}$ to user k for $\forall k \in \mathcal{K}$ and simultaneously carrying out target sensing, the BS transmits the superimposed communication signals and sensing signal, which is given by

$$\mathbf{x} = \sum_{k \in \mathcal{K}} \mathbf{w}_k s_k + \mathbf{r}. \quad (1)$$

Here, $\mathbf{w}_k \in \mathbb{C}^{N \times 1}$ denotes the beamformer for transmitting the unicast symbol s_k and $\mathbf{r} \in \mathbb{C}^{N \times 1}$ denotes the sensing signal. Without loss of generality, we assume that $\{s_k\}$ are statistically independent with zero mean and unit power. The sensing signal \mathbf{r} is assumed to be independent with the information symbols $\{s_k\}$ and have the covariance matrix $\mathbf{R}_r = \mathbb{E}[\mathbf{r}\mathbf{r}^H] \succeq 0$. Multiple-beam transmission is employed to construct the sensing signal. In this case, the sensing signal can be decomposed into multiple sensing beams via the eigenvalue decomposition:

$$\mathbf{R}_r = \sum_{q=1}^{\text{rank}(\mathbf{R}_r)} \lambda_q \mathbf{v}_q \mathbf{v}_q^H = \sum_{q=1}^{\text{rank}(\mathbf{R}_r)} \mathbf{w}_{r,q} \mathbf{w}_{r,q}^H, \quad (2)$$

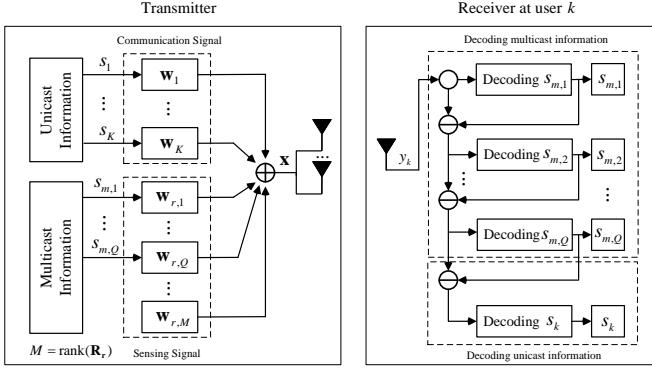


Fig. 2: Block diagram of the transmitter and the receiver at user k in the NOMA-inspired ISAC framework.

where $\lambda_q \in \mathbb{R}$ is the eigenvalue and $\mathbf{v}_q \in \mathbb{C}^{N \times 1}$ is the corresponding eigenvector. The vector $\mathbf{w}_{r,q} = \sqrt{\lambda_q} \mathbf{v}_q$ is the transmit beamformer for the q -th beam of the sensing signal. Without loss of generality, we assume $\lambda_1 \geq \lambda_2 \geq \dots \geq \lambda_{\text{rank}(\mathbf{R}_r)}$. Inspired by NOMA, we embed multicast information into the sensing beam corresponding to the largest $Q \leq \text{rank}(\mathbf{R}_r)$ eigenvalues on the top of the unicast communication signals, as shown in Fig. 2. One example of the practical applications of this transmission scheme is that in the Internet-of-Things (IoT) scenarios, the multicast function can be exploited to broadcast the imaging information of the surrounding environment obtained through radar sensing to a group of IoT devices, while the unicast information can be personalized software updates or the commands for individual IoT devices. In this case, the sensing signal can be rewritten as follows:

$$\mathbf{r} = \sum_{q \in \mathcal{Q}} \mathbf{w}_{r,q} s_{m,q} + \tilde{\mathbf{r}}, \quad (3)$$

where $\mathcal{Q} = \{1, \dots, Q\}$ and $s_{m,q} \in \mathbb{C}$ denotes the independent multicast information symbol with zero mean and unit power. $\tilde{\mathbf{r}}$ denotes the remaining sensing signal without the multicast information, which is assumed to be independent with $\{s_{m,q}\}$ and have the following covariance matrix $\mathbf{R}_{\tilde{\mathbf{r}}}$:

$$\begin{aligned} \mathbf{R}_{\tilde{\mathbf{r}}} &= \mathbb{E} \left[\left(\mathbf{r} - \sum_{q \in \mathcal{Q}} \mathbf{w}_{r,q} s_{m,q} \right) \left(\mathbf{r} - \sum_{q \in \mathcal{Q}} \mathbf{w}_{r,q} s_{m,q} \right)^H \right] \\ &= \sum_{i=Q+1}^{\text{rank}(\mathbf{R}_r)} \mathbf{w}_{r,i} \mathbf{w}_{r,i}^H. \end{aligned} \quad (4)$$

1) *Communication Model*: Given the transmit signal in (1) and (3), the received signal at user k is given by²

$$y_k = \underbrace{\mathbf{h}_k^H \sum_{q \in \mathcal{Q}} \mathbf{w}_{r,q} s_{m,q}}_{\text{multicast/sensing signal}} + \underbrace{\mathbf{h}_k^H \mathbf{w}_k s_{u,k}}_{\text{desired unicast signal}} + \underbrace{\mathbf{h}_k^H \sum_{i \in \mathcal{K}, i \neq k} \mathbf{w}_i s_{u,i}}_{\text{inter-user interference}} + n_k, \quad (5)$$

²Note that the multicast transmission here is different from that in [19] due to the following reasons. Firstly, the multicast transmission in [19] is achieved by the additional multicast signal, while that in this work is based on the existing sensing signal. Secondly, the multicast-unicast framework proposed for the general multiple-user case in [19] is achieved by the cluster-based NOMA, where the available DoFs for target sensing is still limited by the number of communication users according to the analysis in [20]. However, the framework proposed in this work can achieve the full DoFs for target sensing by the sensing signal.

$$+ \underbrace{\mathbf{h}_k^H \tilde{\mathbf{r}}}_{\text{remaining sensing interference}} + n_k, \quad (5)$$

where $\mathbf{h}_k \in \mathbb{C}^{N \times 1}$ denotes the BS-user channel and $n_k \sim \mathcal{CN}(0, \sigma_n^2)$ denotes the CSCG noise with variance σ_n^2 . The decoding procedure is shown in Fig. 2. Following the NOMA protocol, user k successively detects the signals by exploiting SIC, where the multicast streams corresponding to the larger eigenvalues are firstly detected by treating other signals as noise and then removed from the received signal. Thus, the achievable rate of the q -th stream of the multicast signal at user k is given by

$$R_{m,q,k}^N = \log_2 \left(1 + \frac{|\mathbf{h}_k^H \mathbf{w}_{r,q}|^2}{I_{m,q,k} + I_{u \rightarrow m,k} + I_{r,k} + \sigma_n^2} \right), \quad (6)$$

where $I_{m,q,k} = \sum_{i \in \mathcal{Q}, i > q} |\mathbf{h}_k^H \mathbf{w}_{r,i}|^2$ denotes the inter-stream interference of the multicast signal at the SIC receiver, $I_{u \rightarrow m,k} = \sum_{i \in \mathcal{K}} |\mathbf{h}_k^H \mathbf{w}_i|^2$ denotes the interference from the unicast signals to the multicast signal, and $I_{r,k} = \mathbf{h}_k^H \mathbf{R}_{\tilde{\mathbf{r}}} \mathbf{h}_k$ denotes the interference from remaining sensing signal. As the multicast information needs to be delivered to all the K users, the effective achievable rate of the q -th stream of the multicast signal is limited by the user achieving the lowest rate, which is given by

$$R_{m,q}^N = \min\{R_{m,q,1}^N, R_{m,q,2}^N, \dots, R_{m,q,K}^N\}. \quad (7)$$

After decoding and removing all the streams of the multicast signal via SIC, there is no interference from the multicast signal to the unicast signal. Thus, the achievable rate of the unicast signal at user k is given by

$$R_{u,k}^N = \log_2 \left(1 + \frac{|\mathbf{h}_k^H \mathbf{w}_k|^2}{I_{u \rightarrow u,k} + I_{r,k} + \sigma_n^2} \right), \quad (8)$$

where $I_{u \rightarrow u} = \sum_{i \in \mathcal{K}, i \neq k} |\mathbf{h}_k^H \mathbf{w}_i|^2$ denotes the inter-user interference. The communication throughput of the proposed NOMA-inspired ISAC system is the sum rate of the multicast and unicast signals, which is given by

$$R^N = \sum_{q \in \mathcal{Q}} R_{m,q}^N + \sum_{k \in \mathcal{K}} R_{u,k}^N. \quad (9)$$

2) *Sensing Model*: Both communication and sensing signals can be exploited to achieve a desired sensing beampattern, which is the key metric of the radar sensing and can be given by [27]

$$P(\theta_l, \mathbf{R}_x) = \mathbf{a}^H(\theta_l) \mathbf{R}_x \mathbf{a}(\theta_l). \quad (10)$$

Here, $\mathbf{a}(\theta_l) = [1, e^{j \frac{2\pi}{\lambda} d \sin(\theta_l)}, \dots, e^{j \frac{2\pi}{\lambda} d(N-1) \sin(\theta_l)}]^T$ is the steering vector of direction θ_l when the uniform linear array (ULA) is used at the BS. \mathbf{R}_x is transmit covariance matrix, which is given by

$$\begin{aligned} \mathbf{R}_x &= \mathbb{E}[\mathbf{x} \mathbf{x}^H] = \sum_{i \in \mathcal{K}} \mathbf{w}_i \mathbf{w}_i^H + \mathbf{R}_r \\ &= \sum_{i \in \mathcal{K}} \mathbf{w}_i \mathbf{w}_i^H + \sum_{q \in \mathcal{Q}} \mathbf{w}_{r,q} \mathbf{w}_{r,q}^H + \mathbf{R}_{\tilde{\mathbf{r}}}. \end{aligned} \quad (11)$$

In practice, the desired sensing beampattern is designed according to the radar sensing requirements [27]. For example, if the radar sensing system has no information about target

and works in the detecting mode, an isotropic beam pattern is desired, i.e., the power is uniformly distributed among all directions. However, when the radar sensing system has prior information of targets and works in the tracking mode, the beam pattern is expected to have the dominant peak power in the target directions.

Remark 1. The main benefits of the proposed NOMA-inspired ISAC framework can be summarized as follows. Firstly, by embedding the multicast information into part of the sensing signal, the sensing interference on the unicast communication signals can be eliminated via SIC, see (5) and (8). Secondly, the sensing signal is further exploited for facilitating the communication through carrying out multicast transmission, see (3) and (9). Thirdly, the sensing signal provides more DoFs to achieve high quality sensing beam pattern, see (10) and (11). Last but not least, the proposed NOMA-inspired ISAC framework facilitates the *double benefits* of the sensing signal, i.e., enhancing both communication and radar sensing.

Let $\{\phi(\theta_l)\}_{l=1}^L$ denotes a pre-designed sensing beam pattern over an angular grid $\{\theta_l\}_{l=1}^L$ covering the detector's angular range $[-\frac{\pi}{2}, \frac{\pi}{2}]$. The optimal beam pattern for the sensing-only system approximating $\{\phi(\theta_l)\}_{l=1}^L$ can be obtained by solving the following least-square problem [27]:

$$(P0): \min_{\delta, \mathbf{R}_x} \frac{1}{L} \sum_{l=1}^L |\delta \phi(\theta_l) - \mathbf{a}^H(\theta_l) \mathbf{R}_x \mathbf{a}(\theta_l)|^2 \quad (12a)$$

$$\text{s.t.} \quad \text{tr}(\mathbf{R}_x) = P_t, \quad (12b)$$

$$\mathbf{R}_x \succeq 0, \quad (12c)$$

$$\delta \geq 0, \quad (12d)$$

where δ is a scaling parameter and P_t denotes the total transmit power budget. The equality power constraint (12b) is to make BS use all the transmit power to maximize the radar sensing performance [14]. It can be verified that problem (P0) is convex and can be efficiently solved. Let \mathbf{R}_x^* denote the optimal solution to problem (P0). Then, for the ISAC system, the performance of the radar sensing can be evaluated by the following least-square loss function:

$$L(\mathbf{R}_x) = \frac{1}{L} \sum_{l=1}^L |P(\theta_l, \mathbf{R}_x^*) - P(\theta_l, \mathbf{R}_x)|^2. \quad (13)$$

It is worth noting that minimizing $L(\mathbf{R}_x)$ is in conflict with maximizing the communication throughput R^N , especially when radar sensing works in the tracking mode. The reason can be explained as follows. Maximizing the communication throughput requires the high transmit power in the user-desired directions, e.g., the directions of scatters and reflectors in the BS-user channels. However, minimizing $L(\mathbf{R}_x)$ will force the BS to transmit high power in the target directions and low power in the non-target directions. Generally, due to the randomness of the BS-user channel, the user-desired directions have a high probability to fall into the non-target directions. In this case, the tailored transmit beamforming design is required to facilitate both communication and radar sensing simultaneously.

B. Problem Formulation

Given the proposed NOMA-inspired ISAC framework, it is shown in the previous subsection that there are two conflicting objectives, i.e., maximizing the communication throughput and minimizing the beam pattern matching error. For maximizing the communication throughput, the related single-objective optimization problem (SOOP) subject to the total transmit power is formulated as follows:

Problem 1 (Throughput Maximization):

$$(P1): \max_{\mathbf{w}_k, \mathbf{w}_{r,q}, \mathbf{R}_{\bar{\mathbf{r}}}} \sum_{q \in \mathcal{Q}} R_{m,q}^N + \sum_{k \in \mathcal{K}} R_{u,k}^N \quad (14a)$$

$$\text{s.t.} \quad \sum_{k \in \mathcal{K}} \|\mathbf{w}_k\|^2 + \sum_{q \in \mathcal{Q}} \|\mathbf{w}_{r,q}\|^2 + \text{tr}(\mathbf{R}_{\bar{\mathbf{r}}}) \leq P_t, \quad (14b)$$

$$\mathbf{R}_{\bar{\mathbf{r}}} \succeq 0. \quad (14c)$$

Unlike the communication function, the radar sensing function requires the equality power constraint. Thus, the SOOP for the beam pattern matching error minimization is formulated as follows:

Problem 2 (Beam pattern Matching Error Minimization):

$$(P2): \min_{\mathbf{w}_k, \mathbf{w}_{r,q}, \mathbf{R}_{\bar{\mathbf{r}}}} \frac{1}{L} \sum_{l=1}^L |P(\theta_l, \mathbf{R}_x^*) - P(\theta_l, \mathbf{R}_x)|^2 \quad (15a)$$

$$\text{s.t.} \quad \sum_{k \in \mathcal{K}} \|\mathbf{w}_k\|^2 + \sum_{q \in \mathcal{Q}} \|\mathbf{w}_{r,q}\|^2 + \text{tr}(\mathbf{R}_{\bar{\mathbf{r}}}) = P_t, \quad (15b)$$

$$\mathbf{R}_{\bar{\mathbf{r}}} \succeq 0. \quad (15c)$$

Then, based on (P1) and (P2), a multiple-objective optimization problem (MOOP) is formulated for the purpose of investigating the trade-off between the two conflicting objectives, which is given by

Problem 3 (Multiple Objective Optimization):

$$(P3): Q1 : \max_{\mathbf{w}_k, \mathbf{w}_{r,q}, \mathbf{R}_{\bar{\mathbf{r}}}} \sum_{q \in \mathcal{Q}} R_{m,q}^N + \sum_{k \in \mathcal{K}} R_{u,k}^N \quad (16a)$$

$$Q2 : \min_{\mathbf{w}_k, \mathbf{w}_{r,q}, \mathbf{R}_{\bar{\mathbf{r}}}} \frac{1}{L} \sum_{l=1}^L |P(\theta_l, \mathbf{R}_x^*) - P(\theta_l, \mathbf{R}_x)|^2 \quad (16b)$$

$$\text{s.t.} \quad \sum_{k \in \mathcal{K}} \|\mathbf{w}_k\|^2 + \sum_{q \in \mathcal{Q}} \|\mathbf{w}_{r,q}\|^2 + \text{tr}(\mathbf{R}_{\bar{\mathbf{r}}}) = P_t, \quad (16c)$$

$$\mathbf{R}_{\bar{\mathbf{r}}} \succeq 0. \quad (16d)$$

III. PROPOSED SOLUTIONS AND PROPERTY ANALYSIS

In this section, we first propose a double-layer FP-SCA-based BCD algorithm to solve problem (P3) of two conflicting objectives in the general multiple-user scenario. To be specific, we firstly transform problem (P3) to a SOOP by adopting the ϵ -constraint method [28], where Q1 is treated as the main objective while Q2 is transformed into the constraint set. Then, the resultant SOOP is decomposed into three disjoint blocks via the FP methods [29], [30] and solved by exploiting BCD and SCA [31] to obtain a suboptimal solution. Moreover, for the spacial single-user scenario, we obtain a globally optimal solution by treating Q2 as the main objective and transforming Q1 into the constraint. The resultant problem is a convex quadratic semidefinite program (QSDP) and can

be optimally solved. Finally, the property of the proposed framework is analyzed by comparing it with the state-of-the-art ISAC frameworks.

A. Suboptimal Solution to (P3) for the General Multiple-User Scenario

To address the conflicting objectives in (P3), the ϵ -constraint method is exploited, based on which (P3) is transformed into a SOOP as follows:

$$(P3.1): \max_{\mathbf{w}_k, \mathbf{w}_{r,q}, \mathbf{R}_{\bar{r}}} \sum_{q \in \mathcal{Q}} R_{m,q}^N + \sum_{k \in \mathcal{K}} R_{u,k}^N \quad (17a)$$

$$\text{s.t.} \quad \frac{1}{L} \sum_{l=1}^L |P(\theta_l, \mathbf{R}_{\mathbf{x}}^*) - P(\theta_l, \mathbf{R}_{\mathbf{x}})|^2 \leq \epsilon_1, \quad (17b)$$

$$(16c), (16d). \quad (17c)$$

It is worth noting that the whole Pareto frontier of the two objectives can be obtained by varying the value of ϵ_1 and solving the corresponding optimization problem [28]. However, it is general challenging to find the globally optimal solution of (P3.1) since the optimization variables $\{\mathbf{w}_k\}$, $\{\mathbf{w}_{r,q}\}$, and $\mathbf{R}_{\bar{r}}$ are highly coupled in the non-convex objective function (17a) and quadratic equality constraint (16c). As a remedy, we propose a double-layer FP-SCA-based BCD algorithm to obtain a suboptimal solution. To start with, we introduce the auxiliary variables $\mathbf{W}_{r,q} = \mathbf{w}_{r,q} \mathbf{w}_{r,q}^H, \forall q \in \mathcal{Q}$, where $\mathbf{W}_{r,q} \succeq 0$ and $\text{rank}(\mathbf{W}_{r,q}) = 1$, and $\mathbf{W}_k = \mathbf{w}_k \mathbf{w}_k^H, \forall k \in \mathcal{K}$, where $\mathbf{W}_k \succeq 0$ and $\text{rank}(\mathbf{W}_k) = 1$. Then, the transmit covariance matrix in (11) becomes

$$\mathbf{R}_{\mathbf{x}} = \sum_{k \in \mathcal{K}} \mathbf{W}_k + \sum_{q \in \mathcal{Q}} \mathbf{W}_{r,q} + \mathbf{R}_{\bar{r}}. \quad (18)$$

Moreover, the achievable rate of the multicast signal and the unicast signal at user k can be rewritten as

$$R_{m,q,k}^N = \log_2 \left(1 + \frac{\mathbf{h}_k^H \mathbf{W}_{r,q} \mathbf{h}_k}{\tilde{I}_{m,q,k} + \tilde{I}_{u \rightarrow m,k} + I_{r,k} + \sigma_n^2} \right), \quad (19)$$

$$R_{u,k}^N = \log_2 \left(1 + \frac{\mathbf{h}_k^H \mathbf{W}_k \mathbf{h}_k}{\tilde{I}_{u \rightarrow u,k} + I_{r,k} + \sigma_n^2} \right). \quad (20)$$

where $\tilde{I}_{m,q,k} = \sum_{i \in \mathcal{Q}, i > q} \mathbf{h}_k^H \mathbf{W}_{r,i} \mathbf{h}_k$, $\tilde{I}_{u \rightarrow m,k} = \sum_{i \in \mathcal{K}} \mathbf{h}_k^H \mathbf{W}_i \mathbf{h}_k$, and $\tilde{I}_{u \rightarrow u,k} = \sum_{i \in \mathcal{K}, i \neq k} \mathbf{h}_k^H \mathbf{W}_i \mathbf{h}_k$. Then, in order to remove the $\min\{\cdot\}$ function in the multicast rate $R_{m,q}^N$, we transform (P3.1) to an equivalent problem, which is given by

$$(P3.2): \max_{\Theta} f_0(\Theta) = \sum_{q \in \mathcal{Q}} \tilde{R}_{m,q}^N + \sum_{k \in \mathcal{K}} R_{u,k}^N \quad (21a)$$

$$\text{s.t.} \quad R_{m,q,k}^N \geq \tilde{R}_{m,q}^N \geq 0, \forall q \in \mathcal{Q}, \forall k \in \mathcal{K}, \quad (21b)$$

$$\frac{1}{L} \sum_{l=1}^L |P(\theta_l, \mathbf{R}_{\mathbf{x}}^*) - P(\theta_l, \mathbf{R}_{\mathbf{x}})|^2 \leq \epsilon_1, \quad (21c)$$

$$\sum_{k \in \mathcal{K}} \text{tr}(\mathbf{W}_k) + \sum_{q \in \mathcal{Q}} \text{tr}(\mathbf{W}_{r,q}) + \text{tr}(\mathbf{R}_{\bar{r}}) = P_t, \quad (21d)$$

$$\mathbf{W}_{r,q} \succeq 0, \text{rank}(\mathbf{W}_{r,q}) = 1, \forall q \in \mathcal{Q}, \quad (21e)$$

$$\mathbf{W}_k \succeq 0, \text{rank}(\mathbf{W}_k) = 1, \forall k \in \mathcal{K}, \quad (21f)$$

$$\mathbf{R}_{\bar{r}} \succeq 0, \quad (21g)$$

where $\tilde{R}_{m,q}^N \in \mathbb{R}$ is the auxiliary variable and $\Theta = (\tilde{R}_{m,q}^N, \mathbf{W}_k, \mathbf{W}_{r,q}, \mathbf{R}_{\bar{r}})$ denotes all the optimization variables. Next, we reformulated problem (P3.2) by invoking the FP approach proposed in [29] and [30]. Based on FP, (P3.2) can be decomposed into three disjoint blocks and solved iteratively by BCD. Specifically, in BCD, two blocks can be updated with the closed-form expressions and the remaining one can be updated via SCA [31].

1) *FP approach for problem reformulation:* Let $\gamma_{u,k}$ denote the SINR term in $R_{u,k}^N$, i.e., $R_{u,k}^N = \log_2(1 + \gamma_{u,k})$. Then, by applying the Lagrangian dual transform proposed in [30] and introducing an auxiliary variable $\alpha = [\alpha_1, \dots, \alpha_K]^T \in \mathbb{R}^{K \times 1}$, $R_{u,k}^N$ can be transformed to

$$\tilde{R}_{u,k}^N = \log_2(1 + \alpha_k) - \alpha_k + \frac{(1 + \alpha_k)\gamma_{u,k}}{1 + \gamma_{u,k}}. \quad (22)$$

By replacing $R_{u,k}^N$ with $\tilde{R}_{u,k}^N$ in problem (P3.2), we obtain a new optimization problem, which is given by

$$(P3.3): \max_{\alpha, \Theta} f_1(\alpha, \Theta) = \sum_{q \in \mathcal{Q}} \tilde{R}_{m,q}^N + \sum_{k \in \mathcal{K}} \tilde{R}_{u,k}^N \quad (23a)$$

$$\text{s.t.} \quad (21b) - (21e). \quad (23b)$$

Lemma 1. (P3.2) and (P3.3) are equivalent.

Proof. For any given Θ , (P3.3) is an unconstrained convex optimization problem with respect to α and can be rewritten as

$$\alpha^* = \arg \max_{\alpha} f_1(\alpha, \Theta), \quad (24)$$

The optimal α^* can be obtained by

$$\frac{\partial f_1(\alpha, \Theta)}{\partial \alpha_k} = \frac{\partial \tilde{R}_{u,k}^N}{\partial \alpha_k} = 0 \Rightarrow \alpha_k^* = \gamma_{u,k}, \forall k \in \mathcal{K}. \quad (25)$$

For the optimal α^* , it holds that $f_1(\alpha^*, \Theta) = f_0(\Theta)$. Thus, the equivalence between (P3.2) and (P3.3) is guaranteed. ■

Lemma 1 shows the equivalence between (P3.2) and (P3.3). However, the objective function of (P3.3) is still non-convex due to the sum-of-ratio term, which is denoted by

$$\begin{aligned} g(\alpha, \Theta) &= \sum_{k \in \mathcal{K}} \frac{(1 + \alpha_k)\gamma_{u,k}}{1 + \gamma_{u,k}} \\ &= \sum_{k \in \mathcal{K}} \frac{(1 + \alpha_k) \mathbf{h}_k^H \mathbf{W}_k \mathbf{h}_k}{\sum_{i \in \mathcal{K}} \mathbf{h}_k^H \mathbf{W}_i \mathbf{h}_k + \mathbf{h}_k^H \mathbf{R}_{\bar{r}} \mathbf{h}_k + \sigma_n^2}. \end{aligned} \quad (26)$$

Then, the objective function of (P3.3) can be rewritten as

$$f_1(\alpha, \Theta) = \sum_{q \in \mathcal{Q}} \tilde{R}_{m,q}^N + v(\alpha) + g(\alpha, \Theta), \quad (27)$$

where $v(\alpha) = \sum_{k \in \mathcal{K}} (\log_2(1 + \alpha_k) - \alpha_k)$. In order to solve the non-convexity of $g(\alpha, \Theta)$, we transform it into a new function via the quadratic transform proposed in [29], which is given by

$$\begin{aligned} h(\alpha, \beta, \Theta) &= \sum_{k \in \mathcal{K}} \left(2 \text{Re} \left\{ \beta^* \sqrt{(1 + \alpha_k) \mathbf{h}_k^H \mathbf{W}_k \mathbf{h}_k} \right\} \right) \\ &\quad - \sum_{k \in \mathcal{K}} |\beta_k|^2 \left(\sum_{i \in \mathcal{K}} \mathbf{h}_k^H \mathbf{W}_i \mathbf{h}_k + \mathbf{h}_k^H \mathbf{R}_{\bar{r}} \mathbf{h}_k + \sigma_n^2 \right), \end{aligned} \quad (28)$$

where $\boldsymbol{\beta} = [\beta_1, \dots, \beta_K]^T \in \mathbb{C}^{K \times 1}$ is the auxiliary variable. Then, a new optimization problem can be obtained from (P3.3) by replacing $g(\boldsymbol{\alpha}, \boldsymbol{\Theta})$ with $h(\boldsymbol{\alpha}, \boldsymbol{\beta}, \boldsymbol{\Theta})$:

$$(P3.4): \max_{\boldsymbol{\alpha}, \boldsymbol{\beta}, \boldsymbol{\Theta}} f_2(\boldsymbol{\alpha}, \boldsymbol{\beta}, \boldsymbol{\Theta}) = \sum_{q \in \mathcal{Q}} \tilde{R}_{m,q}^N + v(\boldsymbol{\alpha}) + h(\boldsymbol{\alpha}, \boldsymbol{\beta}, \boldsymbol{\Theta}) \quad (29a)$$

$$\text{s.t.} \quad (21b) - (21e). \quad (29b)$$

Lemma 2. (P3.3) and (P3.4) are equivalent.

Proof. For any given $\boldsymbol{\alpha}$ and $\boldsymbol{\Theta}$, (P3.4) is an unconstrained convex optimization with respect to $\boldsymbol{\beta}$ and can be rewritten as

$$\boldsymbol{\beta}^* = \arg \max_{\boldsymbol{\beta}} f_2(\boldsymbol{\alpha}, \boldsymbol{\beta}, \boldsymbol{\Theta}) = \arg \max_{\boldsymbol{\beta}} h(\boldsymbol{\alpha}, \boldsymbol{\beta}, \boldsymbol{\Theta}) + \xi, \quad (30)$$

where ξ denotes all the terms that is not associated with $\boldsymbol{\beta}$. The optimal $\boldsymbol{\beta}^*$ can be obtained by

$$\begin{aligned} \frac{\partial f_2(\boldsymbol{\alpha}, \boldsymbol{\beta}, \boldsymbol{\Theta})}{\partial \beta_k} &= \frac{\partial h(\boldsymbol{\alpha}, \boldsymbol{\beta}, \boldsymbol{\Theta})}{\partial \beta_k} = 0 \quad (31) \\ \Rightarrow \boldsymbol{\beta}_k^* &= \frac{\sqrt{(1 + \alpha_k) \mathbf{h}_k^H \mathbf{W}_k \mathbf{h}_k}}{\sum_{i \in \mathcal{K}} \mathbf{h}_k^H \mathbf{W}_i \mathbf{h}_k + \mathbf{h}_k^H \mathbf{R}_{\bar{r}} \mathbf{h}_k + \sigma_n^2}. \quad (32) \end{aligned}$$

For the optimal $\boldsymbol{\beta}^*$, the equality $h(\boldsymbol{\alpha}, \boldsymbol{\beta}^*, \boldsymbol{\Theta}) = g(\boldsymbol{\alpha}, \boldsymbol{\Theta})$ holds. Thus, the equivalence between (P3.3) and (P3.4) is proved. \blacksquare

According to Lemma 1 and Lemma 2, (P3.2) is equivalent to (P3.4). It can be observed that the optimization variables of problem (P3.4) can be decomposed into three disjoint block $\boldsymbol{\alpha}$, $\boldsymbol{\beta}$, and $\boldsymbol{\Theta}$. Therefore, it can be solved by exploiting BCD through the following procedure:

- 1) Initialize $n = 0$ and a feasible $\boldsymbol{\Theta}^n$;
- 2) Update $\boldsymbol{\alpha}^{n+1}$ by (25) with $\boldsymbol{\Theta}^n$;
- 3) Update $\boldsymbol{\beta}^{n+1}$ by (32) with $\boldsymbol{\alpha}^{n+1}$ and $\boldsymbol{\Theta}^n$;
- 4) Update $\boldsymbol{\Theta}^{n+1}$ by solving (P3.4) with $\boldsymbol{\alpha}^{n+1}$ and $\boldsymbol{\beta}^{n+1}$.

Here, $\boldsymbol{\alpha}^n$, $\boldsymbol{\beta}^n$, and $\boldsymbol{\Theta}^n$ denote the obtained optimization variables in the n -th iterations of BCD. However, despite that the objective function of (P3.4) is concave with respect to $\boldsymbol{\Theta}$ for the fixed $\boldsymbol{\alpha}$ and $\boldsymbol{\beta}$, the constraints (21b), (21e) and (21f) are non-convex, which can be solved by invoking SCA [31].

2) *SCA for updating $\boldsymbol{\Theta}$* : To solve the non-convexity of the constraint (21b), we firstly rewrite $R_{m,q,k}^N$ as follows:

$$R_{m,q,k}^N = \log_2 \left(\mathbf{h}_k^H (\mathbf{A}_q + \mathbf{W}_{r,q}) \mathbf{h}_k + \sigma_n^2 \right) - \underbrace{\log_2 \left(\mathbf{h}_k^H \mathbf{A}_q \mathbf{h}_k + \sigma_n^2 \right)}_{t_{q,k}}, \quad (33)$$

where $\mathbf{A}_q = \sum_{i \in \mathcal{Q}, i > q} \mathbf{W}_{r,q} + \sum_{i \in \mathcal{K}} \mathbf{W}_i + \mathbf{R}_{\bar{r}}$. It can be observed that the non-convexity lies in the term $t_{q,k}$. Let \mathbf{A}_q^n denote the value of \mathbf{A}_q in the n -th iteration of BCD. Then, we adopt a surrogate function $\tilde{t}_{q,k}$ constructed using the first-order Taylor expansion of $t_{q,k}$ at point \mathbf{A}_q^n , which is given by

$$\tilde{t}_{q,k} \triangleq -\log_2 \left(\mathbf{h}_k^H \mathbf{A}_q^n \mathbf{h}_k + \sigma_n^2 \right) - \frac{\mathbf{h}_k^H (\mathbf{A}_q - \mathbf{A}_q^n) \mathbf{h}_k}{\left(\mathbf{h}_k^H \mathbf{A}_q^n \mathbf{h}_k + \sigma_n^2 \right) \ln 2}, \quad (34)$$

As t_k is a convex function of the optimization variables \mathbf{A}_q , the inequality $t_{q,k} \geq \tilde{t}_{q,k}$ holds. Then, $R_{m,q,k}^N$ is bounded by

$$R_{m,q,k}^N \geq \tilde{R}_{m,q,k}^N \triangleq \log_2 \left(\mathbf{h}_k^H (\mathbf{A}_q + \mathbf{W}_{r,q}) \mathbf{h}_k + \sigma_n^2 \right) + \tilde{t}_{q,k}. \quad (35)$$

Therefore, the constraint (21b) can be approximated by $\tilde{R}_{m,q,k}^N \geq \tilde{R}_{m,q}^N \geq 0, \forall q \in \mathcal{Q}, \forall k \in \mathcal{K}$, which is convex.

To solve the non-convex rank-one constraints (21e) and (21f), the semidefinite relaxation (SDR) [32] is generally applied by omitting the rank-one constraint and transforming the original problem to a convex semidefinite program (SDP). In this case, the global optimum of the resultant SDR optimization problem can be efficiently obtained by the convex solvers like CVX [33]. Nevertheless, as the rank-one property of the matrices $\mathbf{W}_{r,i}, \forall i \in \mathcal{M}$ and $\mathbf{W}_k, \forall k \in \mathcal{K}$ is not guaranteed in SDR, the rank-one solutions can be reconstructed via the eigenvalue decomposition or the Gaussian randomization. However, these methods do not ensure the feasibility of the reconstructed rank-one solution and may lead to the performance loss. Therefore, we propose to solve the rank-one constraint by a penalty-based scheme [19], where the rank-one constraints are transformed into a penalty term in the objective function. Firstly, the rank-one constraint can be equivalently transformed into

$$\|\mathbf{W}_{r,q}\|_* - \|\mathbf{W}_{r,q}\|_2 = 0, \forall q \in \mathcal{Q}, \quad (36a)$$

$$\|\mathbf{W}_k\|_* - \|\mathbf{W}_k\|_2 = 0, \forall k \in \mathcal{K}, \quad (36b)$$

where $\|\cdot\|_*$ and $\|\cdot\|_2$ denote the nuclear norm and spectral norm, respectively. The nuclear norm is the sum of all the eigenvalues, while the spectral norm equals to the largest eigenvalue. Thus, for the positive semidefinite matrices $\mathbf{W}_{r,q}$ and \mathbf{W}_k , it holds that $\|\mathbf{W}_{r,q}\|_* - \|\mathbf{W}_{r,q}\|_2 \geq 0$ and $\|\mathbf{W}_k\|_* - \|\mathbf{W}_k\|_2 \geq 0$. Then, the nearly rank-one matrices can be obtained by minimizing the difference between the nuclear norm and spectral norm. Based on this observation, we introduce a penalty term to the objective function of problem (P3.4), which is given by

$$\begin{aligned} \Upsilon(\mathbf{W}_{r,q}, \mathbf{W}_k) &= \sum_{q \in \mathcal{Q}} (\|\mathbf{W}_{r,q}\|_* - \|\mathbf{W}_{r,q}\|_2) \\ &+ \sum_{k \in \mathcal{K}} (\|\mathbf{W}_k\|_* - \|\mathbf{W}_k\|_2). \quad (37) \end{aligned}$$

Then, the new optimization problem with the penalty term for updating $\boldsymbol{\Theta}$ with $\boldsymbol{\alpha}^{n+1}$ and $\boldsymbol{\beta}^{n+1}$ is given as follows:

$$(P3.5): \max_{\boldsymbol{\Theta}} f_2(\boldsymbol{\alpha}^{n+1}, \boldsymbol{\beta}^{n+1}, \boldsymbol{\Theta}) - \frac{1}{\zeta} \Upsilon(\mathbf{W}_{r,q}, \mathbf{W}_k) \quad (38a)$$

$$\text{s.t.} \quad \tilde{R}_{m,q,k} \geq \tilde{R}_{m,q}, \forall k \in \mathcal{K}, \quad (38b)$$

$$(21c) - (21g), \quad (38c)$$

where ζ is the regularization parameter. However, problem (P3.5) is still non-convex due to the terms $-\|\mathbf{W}_{r,q}\|_2$ and $-\|\mathbf{W}_k\|_2$ in the penalty term $\Upsilon(\mathbf{W}_{r,q}, \mathbf{W}_k)$. To solve it, we adopt the surrogate function obtained by the first-order Taylor expansion. Given the point $\mathbf{W}_{r,q}^n$ in the n -th iteration of BCD, the surrogate function $\tilde{\mathbf{W}}_{r,q}^n$ is given by

$$\tilde{\mathbf{W}}_{r,q}^n \triangleq -\|\mathbf{W}_{r,q}^n\|_2 - \text{tr}[\mathbf{u}_{\max,q}^n (\mathbf{u}_{\max,q}^n)^H (\mathbf{W}_{r,q} - \mathbf{W}_{r,q}^n)], \quad (39)$$

where $\mathbf{u}_{\max,q}^n$ denotes the eigenvector corresponding to the largest eigenvalue of the matrix $\mathbf{W}_{r,q}^n$. As $-\|\mathbf{W}_{r,q}\|_2$ is a concave function of the optimization variable $\mathbf{W}_{r,q}$, it holds that $-\|\mathbf{W}_{r,q}\|_2 \leq \widetilde{\mathbf{W}}_{r,q}^n$. The surrogate function $\widetilde{\mathbf{W}}_k^n$ of $-\|\mathbf{W}_k\|_2$ is defined similarly to $\widetilde{\mathbf{W}}_{r,q}^n$. Thus, the penalty term can be approximated by

$$\begin{aligned} \widetilde{\Upsilon}(\mathbf{W}_{r,q}, \mathbf{W}_k) = & \sum_{q \in \mathcal{Q}} (\|\mathbf{W}_{r,q}\|_* + \widetilde{\mathbf{W}}_{r,q}^n) \\ & + \sum_{k \in \mathcal{K}} (\|\mathbf{W}_k\|_* + \widetilde{\mathbf{W}}_k^n), \end{aligned} \quad (40)$$

which yields the following optimization problem:

$$(P3.6): \max_{\Theta} f_2(\alpha^{n+1}, \beta^{n+1}, \Theta) - \frac{1}{\zeta} \widetilde{\Upsilon}(\mathbf{W}_{r,q}, \mathbf{W}_k) \quad (41a)$$

$$\text{s.t.} \quad (38b), (21c) - (21g), \quad (41b)$$

which is a convex QSDP with respect to Θ and can be solved by convex solvers such as CVX [33]. It is pointed out in [34] that the BCD method can converge to a stationary point though the SCA is exploited.

It is worth noting that the value of the regularization parameter ζ has significant influence on the obtained solutions. Specifically, in order to ensure the nearly rank-one solutions, the value of ζ should be sufficient small, i.e., $\zeta \rightarrow 0$ and $1/\zeta \rightarrow +\infty$. However, the objective function is dominated by the penalty term in this case, thereby leading to the insufficiency of maximizing the communication throughput. Therefore, we firstly set ζ to a large value for obtaining a good start point with respect to the communication throughput. Then, the value of ζ is gradually reduced to a sufficiently small value for obtaining a rank-one solution of $\mathbf{W}_{r,q}, \forall q \in \mathcal{Q}$ and $\mathbf{W}_k, \forall k \in \mathcal{K}$. To this end, we introduce an outer layer nested with the inner BCD layer, where the parameter ζ is updated following

$$\zeta = \rho\zeta, 0 < \rho < 1. \quad (42)$$

Based on the approaches proposed above, problem (P3) can be solved in the double-layer iterations. In the inner layer, problem (P3) is transformed to (P3.6) and solved through BCD and SCA with the fixed ζ . In the outer layer, the value of ζ is gradually decreased to ensure a rank-one solution. The inner layer is terminated when the communication throughput of the system converges, i.e.,

$$|(R^N)^n - (R^N)^{n-1}| \leq \tau_1, \quad (43)$$

where $(R^N)^n$ and $(R^N)^{n-1}$ are the throughput in the n -th and $(n-1)$ -th inner iterations, respectively, while the outer layer is terminated when the penalty term is smaller than a pre-defined threshold, i.e.,

$$\Upsilon(\mathbf{W}_{r,q}, \mathbf{W}_k) \leq \tau_2. \quad (44)$$

The detailed algorithm for solving problem (P3) is summarized in Algorithm 1. The computational burden of this algorithm mainly arise from updating α , updating β and solving the QSDP (P3.6), the computational complexity of which are $\mathcal{O}(KN^2)$, $\mathcal{O}(KN^2)$, and $\mathcal{O}((K+Q+1)^{6.5}N^{6.5}\log(1/e))$, respectively. The parameter e denotes the solution accuracy

Algorithm 1 Proposed double-layer FP-SCA-based BCD algorithm for solving problem (P3).

- 1: Choose a non-zero value of ϵ_1 .
 - 2: Initialize the feasible Θ^0 and the parameter ζ .
 - 3: Calculate the communication throughput $(R^N)^0$ based on the given Θ^0 .
 - 4: **repeat**
 - 5: Set iteration index $n = 0$ for inner layer.
 - 6: **repeat**
 - 7: Update α^{n+1} by (25) with Θ^n .
 - 8: Update β^{n+1} by (32) with α^{n+1} and Θ^n .
 - 9: Update Θ^{n+1} by solving (P3.6) with α^{n+1} , β^{n+1} , and Θ^n .
 - 10: $n = n + 1$.
 - 11: **until** $|(R^N)^n - (R^N)^{n-1}| \leq \tau_1$.
 - 12: $\Theta^0 = \Theta^n$, $\zeta = \rho\zeta$.
 - 13: **until** $\Upsilon(\mathbf{W}_{r,q}, \mathbf{W}_k) \leq \tau_2$.
-

for the QSDP using the primal-dual interior-point algorithm. Thus, for I_i inner iterations and I_o outer iterations, the overall complexity of Algorithm 1 is $\mathcal{O}(I_o I_i ((K+Q+1)^{6.5} N^{6.5} \log(1/e) + 2KN^2))$.

B. Globally Optimal Solution to (P3) for the Special Single-User Scenario

The single-user scenario is a special case of the general multiple user scenario with $K = 1$. Thus, the related MOOP can also be suboptimally solved using Algorithm 1. However, in this subsection, we obtain the globally optimal solution of the MOOP in the single user scenario by equivalently transform it to a convex QSDP. Firstly, in the single user scenario, the communication throughput R^N in (9) is reduced to

$$\begin{aligned} R^N = & \sum_{q \in \mathcal{Q}} \log_2 \left(1 + \frac{\mathbf{h}^H \mathbf{W}_{r,q} \mathbf{h}}{\mathbf{h}^H \mathbf{B}_q \mathbf{h} + \mathbf{h}^H \mathbf{W} \mathbf{h} + \mathbf{h}^H \mathbf{R}_{\bar{r}} \mathbf{h} + \sigma_n^2} \right) \\ & + \log_2 \left(1 + \frac{\mathbf{h}^H \mathbf{W} \mathbf{h}}{\mathbf{h}^H \mathbf{R}_{\bar{r}} \mathbf{h} + \sigma_n^2} \right) \\ \stackrel{(a)}{=} & \log_2 \left(1 + \frac{\mathbf{h}^H (\sum_{q \in \mathcal{Q}} \mathbf{W}_{r,q} + \mathbf{W}) \mathbf{h}}{\mathbf{h}^H \mathbf{R}_{\bar{r}} \mathbf{h} + \sigma_n^2} \right) \\ = & \log_2 \left(1 + \frac{\mathbf{h}^H (\mathbf{R}_{\mathbf{x}} - \mathbf{R}_{\bar{r}}) \mathbf{h}}{\mathbf{h}^H \mathbf{R}_{\bar{r}} \mathbf{h} + \sigma_n^2} \right), \end{aligned} \quad (45)$$

where $\mathbf{h} = \mathbf{h}_1$, $\mathbf{B}_q = \sum_{i \in \mathcal{Q}, i > q} \mathbf{W}_{r,i}$, and $\mathbf{W} = \mathbf{W}_1$. The equality (a) is due to the fact that $\log_2(1 + \frac{A}{B+C}) + \log_2(1 + \frac{B}{C}) = \log_2(1 + \frac{A+B}{C})$. It can be observed from (45) that if one more beam of the sensing signal is exploited for transmitting information, the value of $\mathbf{h}^H \mathbf{R}_{\bar{r}} \mathbf{h}$ will be decreased, i.e., less interference power. Meanwhile, the value of $\mathbf{h}^H (\mathbf{R}_{\mathbf{x}} - \mathbf{R}_{\bar{r}}) \mathbf{h}$ will be increased accordingly, i.e., more effective communication power. Therefore, through the proposed NOMA-inspired scheme, we can transform all the interference power to the effective communication power to obtain the maximum communication throughput when all the beams of the sensing signal are exploited to transmit

information. In this case, the communication throughput R^N becomes $R^N = \log_2 \left(1 + \frac{\mathbf{h}^H \mathbf{R}_x \mathbf{h}}{\sigma_n^2} \right)$. The related MOOP is given by

$$(P4): Q1 : \max_{\mathbf{R}_x} \log_2 \left(1 + \frac{\mathbf{h}^H \mathbf{R}_x \mathbf{h}}{\sigma_n^2} \right), \quad (46a)$$

$$Q2 : \min_{\mathbf{R}_x} \frac{1}{L} \sum_{l=1}^L |P(\theta_l, \mathbf{R}_x^*) - P(\theta_l, \mathbf{R}_x)|^2 \quad (46b)$$

$$\text{s.t. } \text{tr}(\mathbf{R}_x) = P_t, \quad (46c)$$

$$\mathbf{R}_x \succeq 0. \quad (46d)$$

Then, by exploiting the ϵ -constraint method, the resultant SOOP for a specific value of ϵ_2 is given by

$$(P4.1): \min_{\mathbf{R}_x} \frac{1}{L} \sum_{l=1}^L |P(\theta_l, \mathbf{R}_x^*) - P(\theta_l, \mathbf{R}_x)|^2 \quad (47a)$$

$$\text{s.t. } \mathbf{h}^H \mathbf{R}_x \mathbf{h} - (2^{\epsilon_2} - 1) \sigma_n^2 \geq 0, \quad (47b)$$

$$(46c), (46d). \quad (47c)$$

It is clear that problem (P4.1) is a convex QSDP and can be optimally solved by the convex solvers like CVX [33]. When the primal-dual interior-point algorithm is exploited, (P4.1) can be solved with the worst complexity of $\mathcal{O}(N^{6.5} \log(1/e))$, where e denotes the solution accuracy.

C. Performance Comparison with the State-of-the-Art ISAC Frameworks

In this subsection, we compare the proposed NOMA-inspired ISAC framework with the state-of-the-art ISAC frameworks, based on which the property of the proposed framework is analyzed.

1) *State-of-the-Art ISAC Frameworks*: In the state-of-the-art ISAC frameworks, the sensing signal is regarded as the harmful interference to communication. Thus, the received signal at user k is given by

$$y_k = \underbrace{\mathbf{h}_k^H \mathbf{w}_k s_{u,k}}_{\text{desired unicast signal}} + \underbrace{\mathbf{h}_k^H \sum_{i \in \mathcal{K}, i \neq k} \mathbf{w}_i s_{u,i}}_{\text{inter-user interference}} + \underbrace{\mathbf{h}_k^H \mathbf{r}}_{\text{sensing interference}} + n_k. \quad (48)$$

The achievable rate of the desired unicast signal at user k is given by

$$R_{u,k}^C = \log_2 \left(1 + \frac{|\mathbf{h}_k^H \mathbf{w}_k|^2}{\sum_{i \in \mathcal{K}, i \neq k} |\mathbf{h}_k^H \mathbf{w}_i|^2 + p \mathbf{h}_k^H \mathbf{R}_r \mathbf{h}_k + \sigma_n^2} \right), \quad (49)$$

where the parameter p is the indicator of the following two state-of-the-art ISAC frameworks:

- **No sensing interference cancellation (No-SenIC) ISAC** [20], [21]: The communication receiver has no capability to mitigate the sensing interference. Thus, the desired unicast signal is decoded subject to the interference from the sensing signal. In this case, $p = 1$.
- **Ideal sensing interference cancellation (Ideal-SenIC) ISAC** [22]: The communication receiver is assumed to

be capable of ideally removing the sensing interference from y_k . In this case, $p = 0$.

2) *General Multiple-user Scenario*: Following the same procedure in Section III-A, in the multiple-user scenario, the SOOP for the Ideal-SenIC ISAC and No-SenIC ISAC obtained by the ϵ -constraint method is given by

$$(P5.1): \max_{\mathbf{w}_k, \mathbf{R}_r} R^C = \sum_{k \in \mathcal{K}} R_{u,k}^C \quad (50a)$$

$$\text{s.t. } \frac{1}{L} \sum_{l=1}^L |P(\theta_l, \mathbf{R}_x^*) - P(\theta_l, \mathbf{R}_x)|^2 \leq \epsilon_1, \quad (50b)$$

$$\sum_{k \in \mathcal{K}} \|\mathbf{w}_k\|^2 + \text{tr}(\mathbf{R}_r) = P_t, \quad (50c)$$

$$\mathbf{R}_r \succeq 0. \quad (50d)$$

Despite the non-convexity of the problem (P5.1), it can be solved by the proposed Algorithm 1 by removing the multicast transmission and considering the interference term in (49). In the following, we compare the NOMA-inspired ISAC frameworks with the Ideal-SenIC and No-SenIC ISAC by analyzing the solution of (P3.1) and (P5.1).

Proposition 1. Given a specific value of ϵ_1 , let \bar{R}^N , \bar{R}^{C0} , and \bar{R}^{C1} denote the optimal values of problem (P3.1), (P5.1) with $p = 0$, and (P5.1) with $p = 1$, respectively. Then, the following equality holds when $Q = N$:

$$\bar{R}^N \geq \bar{R}^{C0} \geq \bar{R}^{C1}. \quad (51)$$

Proof. See Appendix A. ■

Remark 2. Proposition 1 shows that when the same sensing beampattern accuracy is achieved, the proposed NOMA-inspired ISAC framework can achieve the higher communication throughput compared to the existing Ideal-SenIC ISAC and No-SenIC ISAC frameworks, which indicates the benefits of further exploiting the sensing signal for communication. Furthermore, although the inequalities (51) is proved under a strong condition $Q = N$, our numerical results provided in the next section show that $Q = 1$ is sufficient.

3) *Special Single-user Scenario*: For the special single-user scenario, the corresponding SOOP of Ideal-SenIC and No-SenIC ISAC can be obtained following the same procedure in Section III-B, which is given by

$$(P6.1): \min_{\mathbf{W}, \mathbf{R}_r} L(\mathbf{R}_x) = \frac{1}{L} \sum_{l=1}^L |P(\theta_l, \mathbf{R}_x^*) - P(\theta_l, \mathbf{R}_x)|^2 \quad (52a)$$

$$\text{s.t. } \mathbf{h}^H \mathbf{W} \mathbf{h} - (2^{\epsilon_2} - 1) (p \mathbf{h}^H \mathbf{R}_r \mathbf{h} + \sigma_n^2) \geq 0, \quad (52b)$$

$$\text{tr}(\mathbf{W}) + \text{tr}(\mathbf{R}_r) = P_t, \quad (52c)$$

$$\mathbf{W} \succeq 0, \mathbf{R}_r \succeq 0, \quad (52d)$$

where $\mathbf{W} = \mathbf{w} \mathbf{w}^H$. Problem (P6.1) is convex for both $p = 0$ and $p = 1$ and thus can be optimally solved. Although the rank-one constraint of \mathbf{W} is omitted in problem (P6.1), there always exists a globally optimal rank-one solution according to [22, Proposition 1] and [22, Proposition 2].

Proposition 2. Given a specific value of ϵ_2 , let $\bar{\mathbf{R}}_{\mathbf{x}}^N$, $\bar{\mathbf{R}}_{\mathbf{x}}^{C0}$, and $\bar{\mathbf{R}}_{\mathbf{x}}^{C1}$ denote the globally optimal transmit covariance matrix to (P4.1), (P6.1) with $p = 0$, and (P6.1) with $p = 1$, respectively. Then, the following equality holds:

$$L(\bar{\mathbf{R}}_{\mathbf{x}}^N) = L(\bar{\mathbf{R}}_{\mathbf{x}}^{C0}) = L(\bar{\mathbf{R}}_{\mathbf{x}}^{C1}). \quad (53)$$

Proof. See Appendix B. \blacksquare

Remark 3. Proposition 2 indicates that the proposed NOMA-inspired ISAC achieves the same optimal performance as the existing SenIC ISAC frameworks in the single-user scenario, which provides the following insights. On the one hand, there is no need of exploiting the sensing signal to transmit information in the single-user scenario. On the other hand, when only one communication user is served, the ISAC system can always achieve the optimal performance regardless of the capability of the sensing interference cancellation at the receiver. Thus, sensing interference coordination is not needed.

IV. NUMERICAL RESULTS

In this section, the numerical results are provided for characterizing the proposed NOMA-inspired ISAC framework. We assume a dual-functional BS equipped with an ULA with half wavelength spacing, which works in the tracking mode to sensing 3 targets in the directions $\Phi = \{-60^\circ, 0^\circ, 60^\circ\}$. Given the directions of sensing targets, the desired beam pattern is given by

$$\phi(\theta_l) = \begin{cases} 1, & \theta_l \in [\varphi - \frac{\Delta}{2}, \varphi + \frac{\Delta}{2}], \forall \varphi \in \Phi, \\ 0, & \text{otherwise,} \end{cases} \quad (54)$$

where Δ is the desired beam width, which is set to 10° in the simulation, and the angle grid $\{\theta_l\}_{l=1}^L$ is set to $[-\frac{\pi}{2} : \frac{\pi}{100} : \frac{\pi}{2}]$. The transmit power budget at BS and the noise power at the communication users are set to $P_t = 20$ dBm and $\sigma_n^2 = -80$ dBm, respectively. The channels between BS and communication users are assumed to experience Rayleigh fading and 80 dB path loss.

A. Multiple User Scenario

In this section, numerical results of the multiple-user scenario is presented. We set $N = 8$ and $K = 5$. For Algorithm 1, the initial penalty factor is set to $\zeta = 10^2$ and its reduction factor is set to $\rho = 0.2$. The convergence thresholds of the inner and outer iterations are set to $\tau_1 = 10^{-2}$ and $\tau_2 = 10^{-4}$, respectively.

1) *Benchmark schemes:* Apart from Ideal-SenIC ISAC and No-SenIC ISAC, we also consider the following benchmark schemes for comparison.

- **Communication signal only (Com) ISAC** [15], [16]: In this scheme, the BS only transmits the communication signals for achieving both communication and radar sensing. Thus, the covariance matrix of the transmit signal is $\mathbf{R}_{\mathbf{x}} = \sum_{i \in \mathcal{K}} \mathbf{w}_i \mathbf{w}_i^H$. The achievable at user k is given by

$$R_k^{Com} = \log_2 \left(1 + \frac{|\mathbf{h}_k^H \mathbf{w}_k|^2}{\sum_{i \in \mathcal{K}, i \neq k} |\mathbf{h}_k^H \mathbf{w}_i|^2 + \sigma_n^2} \right). \quad (55)$$

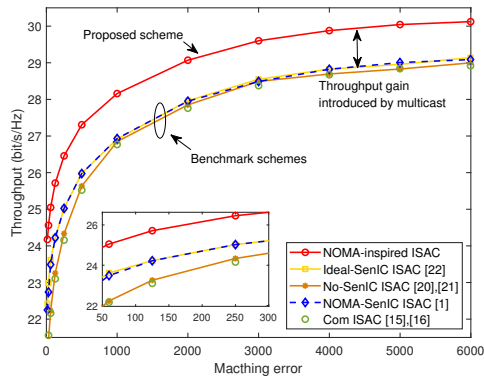


Fig. 3: Trade-off region in the multiple-user scenario with $Q = 1$.

The communication throughput is given by $R^{Com} = \sum_{k \in \mathcal{K}} R_k^{Com}$. The resultant MOOP in the multiple user scenario can be solved by the proposed Algorithm 1.

- **NOMA-inspired sensing interference cancellation (NOMA-SenIC) ISAC** [1]: This scheme is essentially the proposed framework without multicast transmission. In this scheme, the information embedded into the sensing signal is merely used to carry out SIC. In this case, the communication throughput is $R^{N0} = \sum_{k \in \mathcal{K}} R_k^N$. The resultant MOOP can also be solved by the proposed Algorithm 1.

2) *Trade-off Region:* In Fig. 3, the trade-off region between the communication throughput and the beam pattern matching error is studied, which is obtained by averaging over 50 random channel realizations for each scheme. For the proposed NOMA-inspired ISAC framework, we set $Q = 1$. It can be seen that the proposed NOMA-inspired ISAC framework achieves larger trade-off region than the other benchmark schemes. In particular, although only one beam of the sensing signal is exploited to transmit the multicast information, the NOMA-inspired ISAC still significantly outperforms the Ideal-SenIC ISAC. The reason behind this can be explained as follows. The obtained sensing signal is dominated by the beam corresponding to the largest eigenvalue, which can be used to carry the multicast information for achieving considerable rate. Meanwhile, the other beams of the sensing signal have very low power, thus making negligible interference on the communication. This fact is also revealed by the result achieved by the NOMA-SenIC ISAC framework, where even only one beam of the sensing signal is eliminated but the achieved performance is close to that of Ideal-SenIC ISAC. Finally, the No-SenIC ISAC and Com-ISAC frameworks have the worst performance due to the sensing interference and the lack of transmit DoFs, respectively. These results are consistent with **Proposition 1** and **Remark 2**.

3) *Sensing Beam pattern:* In Fig. 4, the sensing beam patterns obtained via different schemes over one channel realization when $R = 26.4$ bit/s/Hz and $Q = 1$ are depicted. One can observe that the proposed NOMA-inspired ISAC framework is capable of achieving the best sensing beam pattern, where there is a noticeable gain of power in the target directions and less power leakage in the undesired directions. When there

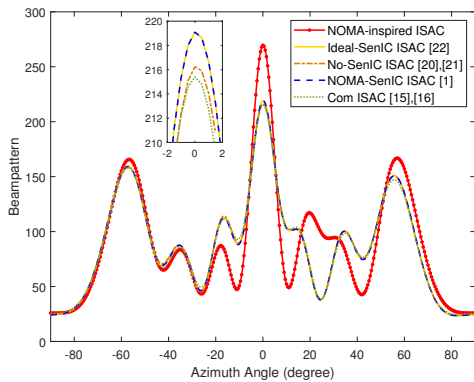


Fig. 4: Obtained sensing beampattern in the multiple-user scenario with throughput $R = 26.4$ bit/s/Hz, $Q = 1$ and $\mu = 0$.

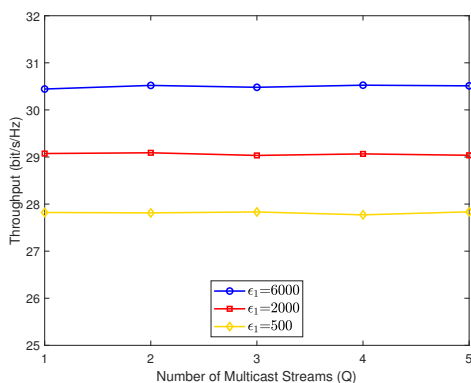


Fig. 5: Communication throughput versus the number of multicast streams.

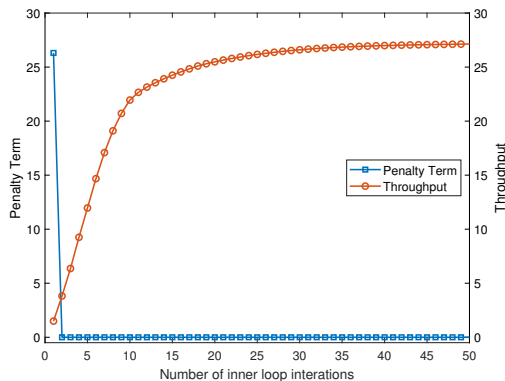


Fig. 6: Convergence of Algorithm 1 when $Q = 1$ and $\epsilon = 2 \times 10^3$.

is no multicast transmission, i.e., in NOMA-SenIC ISAC, the beampattern is still close to the that implemented by the Ideal-SenIC ISAC framework. Additionally, the No-SenIC ISAC and Com-SenIC ISAC frameworks have the largest beampattern distortion.

4) *Throughput versus Q* : In Fig. 5, the relationship between the communication throughput and the number of the multicast-information-bearing sensing beams Q is investigated. The results are obtained by averaging over 50 random channel realizations. It is clear that when the value of Q increases, namely more beams of the sensing signal

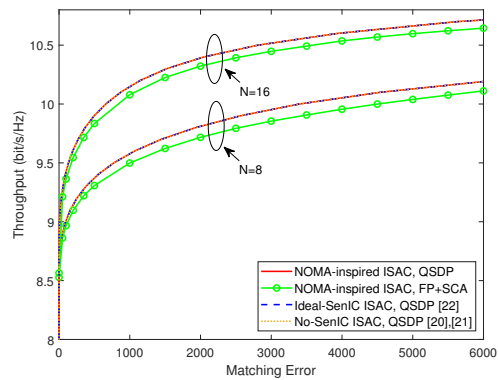


Fig. 7: Trade-off region in the single user scenario.

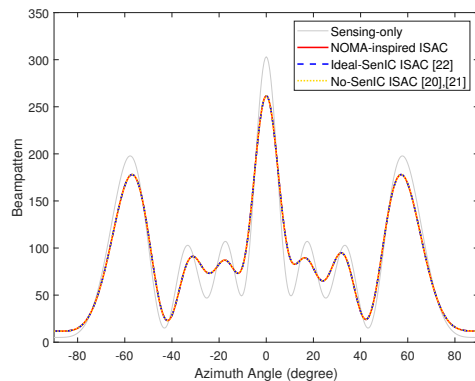


Fig. 8: Obtained transmit beampattern in the single user scenario with $N = 8$ and throughput $R = 9.0$ bit/s/Hz

are exploited to transmit the multicast information and fewer beams have interference on communication, the communication throughput is almost unchanged. This further verifies that the power of sensing signal is mainly concentrated in the beam corresponding to the largest eigenvalue and other beams have negligible interference on communication. Thus, the simplest design of the proposed NOMA-inspired ISAC framework with $Q = 1$ is sufficient in practice.

5) *Convergence of Algorithm 1*: In Fig. 6, we demonstrate the convergence behavior of the proposed algorithm over one random channel realization when $Q = 1$ and $\epsilon = 2 \times 10^3$. We can observe that the throughput gradually increases to stable value, while penalty value quickly converges to almost zero as the number of inner iterations increases, which indicates that the resultant beamformers are rank-one.

B. Single-User Scenario

In this section, the numerical results of the single user scenario is presented, where the proposed NOMA-inspired ISAC is compared with the existing Ideal-SenIC ISAC and No-SenIC ISAC.

1) *Trade-off Region*: In Fig. 7, we investigate the trade-off region of the communication throughput and the beampattern matching error, which is obtained by averaging over one random channel realization. It can be observed that compared to the suboptimal solution obtained via Algorithm 1, the globally optimal solution via QSDP achieves better trade-off

region. Furthermore, one can see that the proposed NOMA-inspired ISAC achieve exactly the same trade-off region as the existing Ideal-SenIC ISAC and No-SenIC ISAC, which is consistent with **Proposition 2** and **Remark 3**.

2) *Sensing Beampattern*: In Fig. 8, we study the obtained sensing beampattern over one random channel realization by NOMA-inspired ISAC, Ideal-SenIC ISAC, and the No-SenIC ISAC when the communication throughput is $R = 9.0$ bit/s/Hz. We set $N = 8$. It can be observed that all the three frameworks can achieve dominant peaks in the target directions. Furthermore, the transmit beampatterns achieved by them are exactly the same, which is also consistent with **Proposition 2** and **Remark 3**.

V. CONCLUSION

In this paper, a NOMA-inspired ISAC framework was proposed, where the transmit sensing signal at BS was further exploited for conveying the multicast information following the concept of NOMA. A tailor-made MOOP designing the transmit beamforming was formulated with the aim of maximizing the communication throughput and minimizing the sensing beampattern matching error. For the multiple-user scenario, the formulated MOOP was transformed to a SOOP via ϵ -constraint method and solved by the proposed double-layer FP-SCA-based BCD algorithm. For the special-single user scenario, the globally optimal solution was obtained by transforming the MOOP to a convex QSDP. It was shown by the theoretical and numerical results that the trade-off region and sensing beampattern are achieved by the proposed NOMA-inspired ISAC in the multiple-user scenario are better than those achieved by the existing SenIC ISAC frameworks, while becoming the same in the single-user scenario. Finally, it was revealed that using only one beam of the sensing signal to convey multicast information still have very high efficiency.

APPENDIX

A. Proof of Proposition 1

Firstly, let $(\{\check{\mathbf{w}}_k\}, \check{\mathbf{R}}_{\mathbf{r}})$ denote any feasible solutions to (P5.1). Then, it holds that

$$\begin{aligned} \check{R}_{u,k}^{C0} &= \log_2 \left(1 + \frac{|\mathbf{h}_k^H \check{\mathbf{w}}_k|^2}{\sum_{i \in \mathcal{K}, i \neq k} |\mathbf{h}_k^H \check{\mathbf{w}}_i|^2 + \sigma_n^2} \right) \\ &\geq \log_2 \left(1 + \frac{|\mathbf{h}_k^H \check{\mathbf{w}}_k|^2}{\sum_{i \in \mathcal{K}, i \neq k} |\mathbf{h}_k^H \check{\mathbf{w}}_i|^2 + \mathbf{h}_k^H \check{\mathbf{R}}_{\mathbf{r}} \mathbf{h}_k + \sigma_n^2} \right) = \check{R}_{u,k}^{C1}, \end{aligned} \quad (56)$$

which is due to the fact that the matrix $\check{\mathbf{R}}_{\mathbf{r}}$ is positive semidefinite. Thus, we have

$$\check{R}^{C0} = \sum_{k \in \mathcal{K}} \check{R}_{u,k}^{C0} \geq \sum_{k \in \mathcal{K}} \check{R}_{u,k}^{C1} = \check{R}^{C1}. \quad (57)$$

Then, when $Q = N$, we define the $\check{\mathbf{w}}_{r,q}, \forall q \in \mathcal{Q}$ as follows:

$$\check{\mathbf{w}}_{r,q} = \begin{cases} \sqrt{\check{\lambda}_q} \check{\mathbf{v}}_q, & 0 \leq q \leq \text{rank}(\check{\mathbf{R}}_{\mathbf{r}}) \\ \mathbf{0}_{N \times 1}, & \text{rank}(\check{\mathbf{R}}_{\mathbf{r}}) < q \leq N \end{cases}, \quad (58)$$

where $\check{\lambda}_q$ and $\check{\mathbf{v}}_q$ are the q -th eigenvalue and eigenvector of $\check{\mathbf{R}}_{\mathbf{r}}$, respectively. Then, it can be verified that $(\{\check{\mathbf{w}}_k\}, \{\check{\mathbf{w}}_{r,q}\}, \check{\mathbf{R}}_{\mathbf{r}} = \mathbf{0}_{N \times N})$ is feasible solutions to (P3.1). As a result, the achievable unicast rate in (P3.1) is given by

$$\check{R}_{u,k}^N = \log_2 \left(1 + \frac{|\mathbf{h}_k^H \check{\mathbf{w}}_k|^2}{\sum_{i \in \mathcal{K}, i \neq k} |\mathbf{h}_k^H \check{\mathbf{w}}_i|^2 + \sigma_n^2} \right) = \check{R}_{u,k}^{C0}. \quad (59)$$

The multicast rate $\check{R}_{m,q}^N \geq 0, \forall q \in \mathcal{Q}$ in (P3.1) can be calculated according to (6) and (7). Thus, it holds that

$$\check{R}^N = \sum_{q \in \mathcal{Q}} \check{R}_{m,q}^N + \sum_{k \in \mathcal{K}} \check{R}_{u,k}^N \geq \sum_{k \in \mathcal{K}} \check{R}_{u,k}^{C0} = \check{R}^{C0}. \quad (60)$$

Based on above analysis, we can conclude that for any feasible solutions $(\{\check{\mathbf{w}}_k\}, \check{\mathbf{R}}_{\mathbf{r}})$ to (P5.1), it always holds that $\check{R}^{C0} \geq \check{R}^{C1}$. Furthermore, there always exists feasible solutions to (P3.1) such that $\check{R}^N \geq \check{R}^{C0}$. Therefore, for the optimal values \bar{R}^N, \bar{R}^{C0} , and \bar{R}^{C1} of the three problems, it must hold that $\bar{R}^N \geq \bar{R}^{C0} \geq \bar{R}^{C1}$ and Proposition 1 is finally proved.

B. Proof of Proposition 2

In order to prove Proposition 2, we firstly give the following three lemmas.

Lemma 3. *Given a specific value of ϵ_2 , it always holds that $L(\bar{\mathbf{R}}_{\mathbf{x}}^{C1}) \geq L(\bar{\mathbf{R}}_{\mathbf{x}}^{C0})$.*

Proof. It can be observed that any feasible solutions to (P6.1) with $p = 1$ are also feasible to (P6.1) with $p = 0$ but not vice versa, which means the feasible region of (P6.1) with $p = 0$ is larger than that of (P6.1) with $p = 1$. Thus, the optimal beampattern matching error achieved by (P6.1) with $p = 0$ is always smaller or equal to that achieved by (P6.1) with $p = 1$ for the same value of ϵ_2 . As a result, Lemma 3 is proved. ■

Lemma 4. *Given a specific value of ϵ_2 , it always holds that $L(\bar{\mathbf{R}}_{\mathbf{x}}^{C0}) \geq L(\bar{\mathbf{R}}_{\mathbf{x}}^N)$.*

Proof. In (P6.1) with $p = 0$, only the communication signal is exploited for communication, while in (P4.1), both communication and sensing signals are exploited for communication. Thus, (P4.1) can be rewritten as

$$(P7.1): \min_{\mathbf{W}, \mathbf{R}_{\mathbf{r}}} L(\mathbf{R}_{\mathbf{x}}) \quad (61a)$$

$$\text{s.t. } \mathbf{h}^H (\mathbf{W} + \mathbf{R}_{\mathbf{r}}) \mathbf{h} - (2^{\epsilon_2} - 1) \sigma_n^2 \geq 0, \quad (61b)$$

$$\text{tr}(\mathbf{W}) + \text{tr}(\mathbf{R}_{\mathbf{r}}) = P_t, \quad (61c)$$

$$\mathbf{W} \succeq \mathbf{0}, \mathbf{R}_{\mathbf{r}} \succeq \mathbf{0}. \quad (61d)$$

It can be observed that any feasible solutions to (P6.1) with $p = 0$ is also feasible to (P7.1) but not vice versa. Thus, Lemma 4 is proved. ■

Lemma 5. *Given a specific value of ϵ_2 , it always holds that $L(\bar{\mathbf{R}}_{\mathbf{x}}^N) = L(\bar{\mathbf{R}}_{\mathbf{x}}^{C1})$.*

Proof. Given the global optimum $\{\mathbf{W}^*, \mathbf{R}_{\mathbf{r}}^*\}$ to (P6.1) with $p = 1$, we now show that $\mathbf{R}_{\mathbf{x}}^* = \mathbf{W}^* + \mathbf{R}_{\mathbf{r}}^*$ is also the global optimum to (P4.1). Firstly, it holds that

$$\mathbf{h}^H \mathbf{R}_{\mathbf{x}}^* \mathbf{h} = \mathbf{h}^H (\mathbf{W}^* + \mathbf{R}_{\mathbf{r}}^*) \mathbf{h} \stackrel{(a)}{\geq} \mathbf{h}^H \mathbf{W}^* \mathbf{h}$$

$$\stackrel{(b)}{\geq} (2^{\epsilon_2} - 1)(\mathbf{h}^H \mathbf{R}_r^* \mathbf{h} + \sigma_n^2) \stackrel{(c)}{\geq} (2^{\epsilon_2} - 1)\sigma_n^2, \quad (62)$$

where (a) and (c) are due to the fact that \mathbf{R}_r^* is positive semidefinite and (b) is due to the feasibility of $\{\mathbf{W}^*, \mathbf{R}_r^*\}$ to (P6.1) with $p = 1$. It also holds that $\text{tr}(\mathbf{R}_x^*) = \text{tr}(\mathbf{W}^* + \mathbf{R}_r^*) = P_t$. Therefore, \mathbf{R}_x^* is a feasible solution to (P4.1).

Furthermore, it can be observed for any feasible solution \mathbf{R}_x to (P4.1), there always exists a solution $\{\mathbf{W} = \mathbf{R}_x, \mathbf{R}_r = \mathbf{0}\}$ that is feasible to (P6.1) with $p = 1$ such that $L(\mathbf{W} + \mathbf{R}_r) = L(\mathbf{R}_x)$. Therefore, it can be shown that

$$L(\mathbf{R}_x^*) = L(\mathbf{W}^* + \mathbf{R}_r^*) \leq L(\mathbf{W} + \mathbf{R}_r) = L(\mathbf{R}_x), \quad (63)$$

which indicates that $\mathbf{R}_x^* = \mathbf{W}^* + \mathbf{R}_r^*$ is a global optimum to (P4.1). Lemma 5 is proved. ■

According to Lemma 3, Lemma 4, and Lemma 5, it is held that $L(\bar{\mathbf{R}}_x^{C1}) \geq L(\bar{\mathbf{R}}_x^{C0}) \geq L(\bar{\mathbf{R}}_x^N) = L(\bar{\mathbf{R}}_x^{C1})$. Thus, the equality among them must be hold and Proposition 2 is finally proved.

REFERENCES

- [1] Z. Wang, Y. Liu, X. Mu, and Z. Ding, "NOMA inspired interference cancellation for integrated sensing and communication," *arXiv preprint arXiv:2112.09207*, 2021.
- [2] K. B. Letaief, W. Chen, Y. Shi, J. Zhang, and Y.-J. A. Zhang, "The roadmap to 6G: AI empowered wireless networks," *IEEE Commun. Mag.*, vol. 57, no. 8, pp. 84–90, Aug. 2019.
- [3] W. Saad, M. Bennis, and M. Chen, "A vision of 6G wireless systems: Applications, trends, technologies, and open research problems," *IEEE Netw.*, vol. 34, no. 3, pp. 134–142, May 2019.
- [4] F. Liu, Y. Cui, C. Masouros, J. Xu, T. X. Han, Y. C. Eldar, and S. Buzzi, "Integrated sensing and communications: Towards dual-functional wireless networks for 6G and beyond," *arXiv preprint arXiv:2108.07165*, 2021.
- [5] Y. Cui, F. Liu, X. Jing, and J. Mu, "Integrating sensing and communications for ubiquitous IoT: Applications, trends and challenges," *IEEE Netw.*, vol. 35, no. 5, pp. 158–167, Nov. 2021.
- [6] T. Wild, V. Braun, and H. Viswanathan, "Joint design of communication and sensing for beyond 5G and 6G systems," *IEEE Access*, vol. 9, pp. 30 845–30 857, Feb. 2021.
- [7] D. K. P. Tan, J. He, Y. Li, A. Bayesteh, Y. Chen, P. Zhu, and W. Tong, "Integrated sensing and communication in 6G: Motivations, use cases, requirements, challenges and future directions," in *Proc. IEEE International Online Symposium on Joint Communications & Sensing (JC&S)*, 2021, pp. 1–6.
- [8] A. R. Chiriyath, B. Paul, and D. W. Bliss, "Radar-communications convergence: Coexistence, cooperation, and co-design," *IEEE Trans. Cogn. Commun. Netw.*, vol. 3, no. 1, pp. 1–12, Mar. 2017.
- [9] J. Guerci, R. Guerci, A. Lackpour, and D. Moskowitz, "Joint design and operation of shared spectrum access for radar and communications," in *Proc. IEEE Radar Conf. (RadarCon)*. IEEE, May 2015, pp. 0761–0766.
- [10] J. Moghaddasi and K. Wu, "Multifunctional transceiver for future radar sensing and radio communicating data-fusion platform," *IEEE access*, vol. 4, pp. 818–838, Feb. 2016.
- [11] G. N. Saddik, R. S. Singh, and E. R. Brown, "Ultra-wideband multifunctional communications/radar system," *IEEE Trans. Microw. Theory Techn.*, vol. 55, no. 7, pp. 1431–1437, Jul. 2007.
- [12] C. Sturm and W. Wiesbeck, "Waveform design and signal processing aspects for fusion of wireless communications and radar sensing," *Proc. IEEE*, vol. 99, no. 7, pp. 1236–1259, Jul. 2011.
- [13] D. Tse and P. Viswanath, *Fundamentals of wireless communication*. Cambridge university press, 2005.
- [14] J. Li and P. Stoica, "MIMO radar with colocated antennas," *IEEE Signal Process. Mag.*, vol. 24, no. 5, pp. 106–114, Sep. 2007.
- [15] F. Liu, C. Masouros, A. Li, H. Sun, and L. Hanzo, "MU-MIMO communications with MIMO radar: From co-existence to joint transmission," *IEEE Trans. Wireless Commun.*, vol. 17, no. 4, pp. 2755–2770, Apr. 2018.
- [16] F. Liu, L. Zhou, C. Masouros, A. Li, W. Luo, and A. Petropulu, "Toward dual-functional radar-communication systems: Optimal waveform design," *IEEE Trans. Signal Process.*, vol. 66, no. 16, pp. 4264–4279, Aug. 2018.
- [17] L. Chen, F. Liu, W. Wang, and C. Masouros, "Joint radar-communication transmission: A generalized pareto optimization framework," *IEEE Trans. Signal Process.*, vol. 69, pp. 2752–2765, May 2021.
- [18] Z. Wang, Y. Liu, X. Mu, Z. Ding, and O. A. Dobre, "NOMA empowered integrated sensing and communication," *IEEE Commun. Lett.*, early access, Jan. 2022, doi:10.1109/LCOMM.2022.3140271.
- [19] X. Mu, Y. Liu, L. Guo, J. Lin, and L. Hanzo, "NOMA-aided joint radar and multicast-unicast communication systems," accepted for the publication in *IEEE J. Sel. Areas Commun.*, 2021, <https://arxiv.org/abs/2110.02372>.
- [20] X. Liu, T. Huang, N. Shlezinger, Y. Liu, J. Zhou, and Y. C. Eldar, "Joint transmit beamforming for multiuser MIMO communications and MIMO radar," *IEEE Trans. Signal Process.*, vol. 68, pp. 3929–3944, Jun. 2020.
- [21] F. Liu, Y.-F. Liu, A. Li, C. Masouros, and Y. C. Eldar, "Cramér-rao bound optimization for joint radar-communication beamforming," *IEEE Transactions on Signal Processing*, vol. 70, pp. 240–253, Dec. 2021.
- [22] H. Hua, J. Xu, and T. X. Han, "Optimal transmit beamforming for integrated sensing and communication," *arXiv preprint arXiv:2104.11871*, 2021.
- [23] X. Liu, T. Huang, and Y. Liu, "Transmit design for joint MIMO radar and multiuser communications with transmit covariance constraint," *arXiv preprint arXiv:2109.00779*, 2021.
- [24] Y. Liu, Z. Qin, M. ElKashlan, Z. Ding, A. Nallanathan, and L. Hanzo, "Non-orthogonal multiple access for 5G and beyond," *Proc. IEEE*, vol. 105, no. 12, pp. 2347–2381, Dec. 2017.
- [25] Y. Liu, H. Xing, C. Pan, A. Nallanathan, M. ElKashlan, and L. Hanzo, "Multiple-antenna-assisted non-orthogonal multiple access," *IEEE Wireless Commun.*, vol. 25, no. 2, pp. 17–23, Apr. 2018.
- [26] Y. Liu, S. Zhang, X. Mu, Z. Ding, R. Schober, N. Al-Dhahir, E. Hossain, and X. Shen, "Evolution of NOMA toward next generation multiple access (NGMA)," *IEEE J. Sel. Areas Commun.*, accepted to appear, 2022. <https://arxiv.org/abs/2108.04561>.
- [27] P. Stoica, J. Li, and Y. Xie, "On probing signal design for MIMO radar," *IEEE Trans. Signal Process.*, vol. 55, no. 8, pp. 4151–4161, Aug. 2007.
- [28] K. Miettinen, *Nonlinear multiobjective optimization*. Springer Science & Business Media, 2012, vol. 12.
- [29] K. Shen and W. Yu, "Fractional programming for communication systems—part I: Power control and beamforming," *IEEE Trans. Signal Process.*, vol. 66, no. 10, pp. 2616–2630, May 2018.
- [30] —, "Fractional programming for communication systems—part II: Uplink scheduling via matching," *IEEE Trans. Signal Process.*, vol. 66, no. 10, pp. 2631–2644, May 2018.
- [31] Y. Sun, P. Babu, and D. P. Palomar, "Majorization-minimization algorithms in signal processing, communications, and machine learning," *IEEE Trans. Signal Process.*, vol. 65, no. 3, pp. 794–816, Feb. 2017.
- [32] Z.-Q. Luo, W.-K. Ma, A. M.-C. So, Y. Ye, and S. Zhang, "Semidefinite relaxation of quadratic optimization problems," *IEEE Signal Process. Mag.*, vol. 27, no. 3, pp. 20–34, May 2010.
- [33] M. Grant and S. Boyd, "CVX: Matlab software for disciplined convex programming, version 2.1," <http://cvxr.com/cvx>, Mar. 2014.
- [34] M. Razaviyayn, M. Hong, and Z.-Q. Luo, "A unified convergence analysis of block successive minimization methods for nonsmooth optimization," *SIAM J. Optim.*, vol. 23, no. 2, pp. 1126–1153, Jun. 2013.